69th International Astronautical Congress (IAC), Bremen, Germany.

IAC–18D1.6.8

Collision detection and isolation for free-floating space robots

Francesco Cavenago[a*], Mauro Massari[a]

[a] *Department of Aerospace Science and Technology, Politecnico di Milano, Via La Masa 34, 20156 Milano, Italy*, francesco.cavenago@polimi.it, mauro.massari@polimi.it
*Corresponding Author

This paper deals with collision handling problem for a free-floating space robot. In future, autonomous satellites equipped with manipulators should be able to perform routine and maintenance work, capture tumbling objects, relocate spacecraft and assembly structures. In these contexts, contacts may occur intentionally or unintentionally. Intelligent robots should be endowed with algorithms to master properly these situations avoiding critical consequences. Collision handling task can be divided into four phases: detection, isolation, identification and reaction. In particular, this paper presents novel techniques to face detection and isolation considering a free-floating space robot. In the free-floating mode, no external forces/torques act on the system and therefore the linear momentum and angular momentum are preserved. When a contact occurs, the momenta lose their stationarity, and thus they are good candidates to be used as monitoring signals to detect a collision. Afterwards, the variation of the momenta is exploited to identify the orientation and point of application of the collision force.

1. Introduction

Even if many efforts have been made in the last thirty years, space robotics is still a novel field of research. Especially, the use of on-orbit manipulators is limited to the Space Shuttle first, followed by the International Space Station experience[1] and few test missions[2][3]. The reason lies in the high risk involved during on-orbit autonomous robotic operations. Hence, further studies are required to enable widespread exploitation of space robots. In future, satellites mounting manipulators could be used to carry out various tasks, such as supporting astronauts in maintenance work, capture of uncooperative objects, assembly of large structures in space, inspection[4]. Moreover, missions involving teams of robots with different tasks could be designed[5].

In these scenarios, dealing with physical contact between the robot and another object is one of the most critical and challenging issue. Many researchers have addressed the problem of guaranteeing a safe interaction during the capture phase in a servicing mission[6][7][8][9]. In this case, the contact at the end-effector is sought intentionally and it can be important to know the impact force as accurately as possible in order to achieve suitable compliant behavior by proper control strategy. The contact can be detected and the force can be measured directly with force sensors duly placed, but they may be inaccurate if the contact does not occur exactly at the foreseen location[6]. Moreover, they make the system more complex and expensive. Therefore, another proposed approach has been to estimate the contact force[6][10].

In this paper, the more general situation of an unexpected collision in an unknown location along the manipulator is considered. Collision handling has been already studied for fixed-base robots, humanoids and flying-robots[11]. As suggested in [11], it can be divided into different phases: detection, isolation, identification and reaction. In the first phase, the occurrence of the collision is detected. Then, in the second and third phases, an estimate of the contact position and force is provided, respectively. In the last phase, the robot is controlled to react properly and avoid critical consequences. Note that intentional contact case is included in this framework since it can be seen as a special case in which the contact position is known *a priori*.

In particular, this work focuses on collision detection and isolation for free-floating space robots. For the detection, the components of the total momentum, which are expected to be constant under unperturbed conditions, are monitored. Especially, a robust change detection test based on intersection of confidence intervals (ICI-CDT [12]) is applied to detect variations in the translational momentum, since it turns out to be particularly noisy, due to the

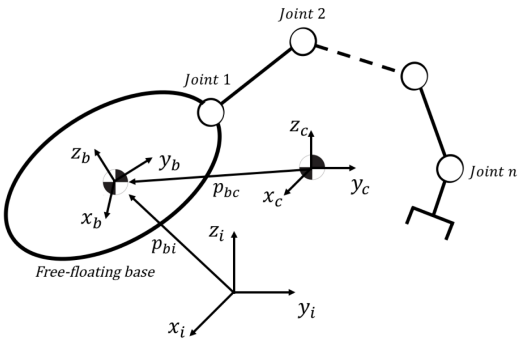

Fig. 1: Free-floating space robot.

dynamics and low measurements accuracy. On the other hand, a simpler threshold approach is used for the rotational momentum, being less noisy thanks to some decoupling achievable by computing it around the center of mass of the whole system. Finally, the second cardinal equation of dynamics is exploited to isolate the collision.

The paper is organized as follows. In Sect. 2, the mathematical model of the free-floating robot is presented. In Sect. 3, a general overview of the collision handling problem is provided. In Sects. 4-5, momentum-based strategies for detection and isolation are proposed and discussed. In Sect. 6, a simulation example is used to assess the performance of the proposed methods. Finally, in Sect. 7 the main conclusions are drawn and future developments are discussed.

2. Space robot modeling

2.1 Assumptions

In this work a space robot composed of rigid bodies connected by rotational joints is considered. No gravitational or environmental disturbances are taken into account, since they are assumed to be less significant in comparison to actuator and inertia torques. It should be noted that these assumptions are commonly accepted in space robotics. Moreover, for what concerns the collision phase, it will be assumed that only one contact at a time occurs on the manipulator.

2.2 Dynamics model of the collision phase

A space robot can be represented as a tree-structured multibody system composed of $n+1$ rigid bodies connected with n joints (see Fig. 1). Considering on-orbit operations, the robot is floating in an inertial space, characterized by a frame denoted by $\mathcal{I}$.

Then, other two reference frames are defined. The first one, denoted by $\mathcal{B}$, is the body frame located on the center of mass (CM) of the robot base. The second one, denoted by $\mathcal{C}$, is a frame with non-rotating axes, parallel to $\mathcal{I}$, placed on the CM of the whole system.

The dynamics of the system can be expressed in $\mathcal{B}$ as follows:

$$\overbrace{\begin{bmatrix} \boldsymbol{M}_t & \boldsymbol{M}_{tr} & \boldsymbol{M}_{tm} \\ \boldsymbol{M}_{tr}^T & \boldsymbol{M}_r & \boldsymbol{M}_{rm} \\ \boldsymbol{M}_{tm}^T & \boldsymbol{M}_{rm}^T & \boldsymbol{M}_m \end{bmatrix}}^{\boldsymbol{M}(\boldsymbol{q})} \begin{bmatrix} \dot{\boldsymbol{v}}_b \\ \dot{\boldsymbol{\omega}}_b \\ \ddot{\boldsymbol{q}} \end{bmatrix} + \underbrace{\begin{bmatrix} \boldsymbol{C}_t & \boldsymbol{C}_{tr} & \boldsymbol{C}_{tm} \\ \boldsymbol{C}_{rt} & \boldsymbol{C}_r & \boldsymbol{C}_{rm} \\ \boldsymbol{C}_{mt} & \boldsymbol{C}_{mr} & \boldsymbol{C}_m \end{bmatrix}}_{\boldsymbol{C}(\boldsymbol{v}_b, \boldsymbol{\omega}_b, \boldsymbol{q}, \dot{\boldsymbol{q}})} \begin{bmatrix} \boldsymbol{v}_b \\ \boldsymbol{\omega}_b \\ \dot{\boldsymbol{q}} \end{bmatrix} = \begin{bmatrix} \boldsymbol{f}_b \\ \boldsymbol{m}_b \\ \boldsymbol{\tau} \end{bmatrix} + \begin{bmatrix} \boldsymbol{f}_{ext,b} \\ \boldsymbol{m}_{ext,b} \\ \boldsymbol{\tau}_{ext} \end{bmatrix} \tag{1}$$

where $\boldsymbol{v}_b, \boldsymbol{\omega}_b \in \mathbb{R}^3$ are the linear and angular velocity of the base; $\boldsymbol{q}, \dot{\boldsymbol{q}} \in \mathbb{R}^n$ are the joint angles and velocities; $\boldsymbol{f}_b, \boldsymbol{m}_b \in \mathbb{R}^3$ are the commanded base force and moment; $\boldsymbol{\tau} \in \mathbb{R}^n$ are the commanded joint torques; $\boldsymbol{f}_{ext,b}, \boldsymbol{m}_{ext,b} \in \mathbb{R}^3$ are the components of the projection in $\mathcal{B}$ of the collision wrench at a generic position, denoted by $\boldsymbol{\mathcal{W}}_{ext} = [\boldsymbol{f}_{ext}^T \, \boldsymbol{m}_{ext}^T]^T \in \mathbb{R}^6$ with $\boldsymbol{f}_{ext}, \boldsymbol{m}_{ext} \in \mathbb{R}^3$ its force and moment, respectively; $\boldsymbol{\tau}_{ext} \in \mathbb{R}^n$ are joint torques caused by the contact; the submatrices $\boldsymbol{M}_t, \boldsymbol{M}_{tr}, \boldsymbol{M}_r \in \mathbb{R}^{3\times3}$ compose the inertia matrix of the system regarded as a composite rigid body; the submatrices $\boldsymbol{M}_{tm}, \boldsymbol{M}_{rm} \in \mathbb{R}^{3\times n}$ compose the coupling inertia matrix; $\boldsymbol{M}_m \in \mathbb{R}^{n\times n}$ is the inertia matrix of the manipulator; $\boldsymbol{C}(\boldsymbol{v}_b, \boldsymbol{\omega}_b, \boldsymbol{q}, \dot{\boldsymbol{q}}) \in \mathbb{R}^{(6+n)\times(6+n)}$ is the Coriolis/centrifugal matrix.

The total generalized momentum, including translational and rotational momentum, around $\mathcal{B}$, denoted by $\boldsymbol{h}_b \in \mathbb{R}^6$, can be written as

$$\boldsymbol{h}_b = \begin{bmatrix} \boldsymbol{M}_t & \boldsymbol{M}_{tr} \\ \boldsymbol{M}_{tr}^T & \boldsymbol{M}_r \end{bmatrix} \begin{bmatrix} \boldsymbol{v}_b \\ \boldsymbol{\omega}_b \end{bmatrix} + \begin{bmatrix} \boldsymbol{M}_{tm} \\ \boldsymbol{M}_{rm} \end{bmatrix} \dot{\boldsymbol{q}} \tag{2}$$

Starting from $\boldsymbol{h}_b$, the total momentum can be computed also around $\mathcal{I}$ and $\mathcal{C}$ as $\boldsymbol{h}_i = \boldsymbol{A}_{ib}^{-T} \boldsymbol{h}_b \in \mathbb{R}^6$ and $\boldsymbol{h}_c = \boldsymbol{A}_{cb}^{-T} \boldsymbol{h}_b \in \mathbb{R}^6$, respectively, exploiting the so-called adjoint transformation matrix:

$$\boldsymbol{A}_{xy} = \begin{bmatrix} \boldsymbol{R}_{xy} & [\boldsymbol{p}_{xy}]^\times \boldsymbol{R}_{xy} \\ \boldsymbol{0} & \boldsymbol{R}_{xy} \end{bmatrix} \in \mathbb{R}^{6\times6} \tag{3}$$

where $\boldsymbol{p}_{xy} \in \mathbb{R}^3$ and $\boldsymbol{R}_{xy} \in \mathbb{R}^{3\times3}$ indicate the generic position vector and rotation matrix from frame $\mathcal{X}$ to frame $\mathcal{Y}$, respectively. The operator $[\,\cdot\,]^\times$ stands for the skew-symmetric matrix of the argument.

Space robots can be operated in three different modes. The base can be fully controlled, only attitude controlled or free to float. In this paper, free-floating robot is considered and thus $\boldsymbol{f}_b$, $\boldsymbol{m}_b$ in Eq. (1) are null and the total momenta $\boldsymbol{h}_i$ and $\boldsymbol{h}_c$ are preserved in absence of external disturbances.

2.3 Measurement model

The measurements of the angular velocity is modeled as[13]:

$$\begin{aligned} \boldsymbol{\omega}_b^m &= \boldsymbol{\omega}_b + \boldsymbol{b}_\omega + \boldsymbol{\eta}_\omega \\ \dot{\boldsymbol{b}}_\omega &= \boldsymbol{\eta}_{b\omega} \end{aligned} \tag{4}$$

where $\boldsymbol{\omega}_b^m \in \mathbb{R}^3$ is the measured angular velocity of the base; the term $\boldsymbol{b}_\omega \in \mathbb{R}^3$ is a bias, considered to be a "Brownian" motion process; the terms $\boldsymbol{\eta}_\omega, \boldsymbol{\eta}_{b\omega} \in \mathbb{R}^3$ are white Gaussian noise with zero mean.

For the other measurements, a white Gaussian noise with zero mean is added to the real values. To be more precise, linear velocity can not be measured directly in practice, but it can be only reconstructed.

3. Collision handling

One of the problem, that must be faced to foster the use of space manipulators, is the handling of physical contact between the robot and another object. Indeed, many applications require the robot to work safely in an environment with other robots, astronauts or passive objects, and to carry out operations in which contact is intentional, e.g. grasping an object, or may occur accidentally. A space robot, with a certain level of autonomy, should be able to collect as much information as possible to get aware of and master effectively these situations, either controlling the post-impact phase or monitoring health status of the system. In the following, a brief overview of the collision handling problem is provided.

Along the same line of [11], collision handling can be divided into different phases: detection, isolation, identification and reaction.

Collision detection: the goal of this phase is to detect whether a collision occurred or not. Basically, a signal, that is expected to behave in a certain way, is monitored and, whenever an unexpected change happens, an alarm is risen. In this phase, it is important to reduce false positive and, at the same time, achieve high sensitivity in order to have a fast detection. Therefore, it is essential to understand the influence of noise and uncertainties on the selected monitoring signal since, as it can be expected, it affects significantly the detection promptness.

Collision isolation: in this phase the part of the robot involved in the collision is identified. This is an important information that can be exploited for both the reaction strategy or health monitoring purposes. Isolation aims at locating the exact point of the collision, or at least the link. Clearly, this phase is required only in case of unexpected collision.

Collision identification: an estimate of the generalized collision force, in terms of direction and intensity, is provided in this phase. The knowledge of the contact force is necessary in order to guarantee a suitable compliant behavior during the post-collision phase, in both intentional or unintentional case. In the latter situation, this information can be exploited also to understand the seriousness of the collision.

Collision reaction: in this last phase the robot should react properly in response to the collision. Depending on the situation, whether the contact is desired or not, different control strategies can be implemented.

In the next paragraphs, the work will focus on the first two phases, namely detection and isolation.

4. Momentum-based collision detection

As already said, a space robot operating in free-floating mode is considered. No external forces and torques act on the system and thus the total momentum is preserved. When the collision occurs, the total momentum components jump from a constant value to another one and therefore they can be exploited as monitoring signals for the detection phase.

In Sect. 2, it has been explained how to compute the total momentum around reference frames $\mathcal{I}$ and $\mathcal{C}$. Under ideal conditions, a contact situation can be detected easily monitoring either $\boldsymbol{h}_i$ or $\boldsymbol{h}_c$ indifferently. However, from practical point of view some considerations should be made. Since on-orbit robotic operations are carried out at relatively low velocity and considering the masses involved, it is reasonable to assume that a collision will cause a relatively small variation in the velocities, especially in the base translational one. In addition, data on linear velocity can be expected to be the most uncertain and thus small changes are difficult to be recognized.

This fact is particularly critical for the translational momentum since the variation of the linear velocity is multiplied by the total mass of the system and, consequently, weights more than the other terms. Hence, small jumps in this momentum are

harder to detect and the detection is more prone to false positive.

As regards the rotational momentum, noise on linear velocity is less critical, but, in any case, it could affect significantly the quality of the signal. Therefore, decoupling the rotational momentum from the linear velocity can be beneficial, guaranteeing a clearer signal to be monitored, and thus prompter detection. This is the reason for preferring $\boldsymbol{h}_c$ to $\boldsymbol{h}_i$; indeed, rotational components of $\boldsymbol{h}_c$ do not depend on the linear velocity. In Sect. 6 some simulations are reported to support this statement.

Depending on the monitored signal, different detection techniques can be exploited. Defining a threshold, below which the modulus of the signal should lie, is the easiest and, probably, the promptest strategy, and for this reason it is exploited to monitor the components of the rotational momentum. An adequate threshold can be defined in the study phase of the mission through simulations, taking into account nonidealities. On the other hand, another approach could be to learn the statistical features of the signal in a training phase directly in orbit and define the threshold as $\mu \pm \Gamma_{th}\sigma$, with μ, σ the mean and standard deviation of the generic signal and Γ_{th} a confidence parameter.

Despite the explained advantages, threshold approach is not particularly robust, in terms of false positive, when dealing with high-noisy signals, like the translational momentum. In this case, a more robust technique has been chosen, named ICI-CDT (Change Detection Test based on Intersection of Confidence Intervals). This strategy is a sequential change detection test that can work with noisy data without *a priori* statistical information about the process, which is acquired in an initial training phase. It exploits the ICI-rule which is a technique that regularizes Gaussian-distributed data through polynomial regression computed on adaptive support. Especially, for change detection test, a 0^{th} oder polynomial is considered since the signal is expected to be stationary.

During the training phase, a training time T_0 is chosen and the available data are windowed in disjoint subsequences composed of N instances. For each subsequence s the sample mean $M(s)$, which is Gaussian distributed thanks to the central limit theorem, is computed. Then, mean and standard deviation of $M(s)$, over the training set composed of $S_0 = T_0/N$ subsequences, are computed. These estimates define the confidence interval for the mean feature that, under stationary condition, can be defined as:

$$\mathscr{I}_{S_0}^M = \left[\mu_{S_0}^M - \Gamma_{cdt}\sigma_{S_0}^M, \mu_{S_0}^M + \Gamma_{cdt}\sigma_{S_0}^M\right] \qquad (5)$$

with $\Gamma_{cdt} > 0$ controlling the amplitude of the interval.

Once the training is completed, the ICI-CDT becomes operational. Every time N data are available, a new sequence s is created and feature extracted to populate $\mathscr{I}_s^M$.

The ICI-rule is used to verify wether the new feature instance can be intended as a realization of the existing distribution. If not, a drift is detected. Basically, it computes the intersection of all the confidence intervals up to the current one and when the result is an empty set a change is detected.

A more comprehensive discussion of these strategies can be found in [12] and [14].

The versatility, namely the possibility to work with both Gaussian ($N = 1$) and non Gaussian noise ($N \geq 20$), and the capability of working with high level of noise, with respect to the signal variation, are the main advantages of the ICI-CDT. This technique has the main drawbacks of having to wait N observations, in case of non Gaussian noise, and, in any case, of a structural delay as time passes. However, the latter disadvantage could be overcome resetting periodically the method, keeping and restarting from the information of the training.

In both strategies, the confidence parameter is used to modify the sensitivity; especially, a tradeoff between detection promptness and robustness to false positive must be made.

As last remark, in order to mitigate the occurrence of false positive, a second layer that validates the detection could be introduced. In this case, the fact that translational and rotational momentum are related to each other could be exploited to this aim. For instance, if a change is detected in some components of the rotational momentum, a change is also expected in the translational momentum and thus this additional information can be used to validate the first detection with a certain degree of confidence.

5. Momentum-based collision isolation

In unexpected collision handling problem, finding the position where the external force is applied is particularly challenging, especially if more than one contact occurs at the same time. In ground applications, dedicated external sensors can be used, such as tactile skin or proximity sensors. However, in case of

space applications, exploiting typical sensing equipment seems to be a better solution, in terms of cost, power and weight.

Assuming that the point of application of the generalized collision force does not change during the collision phase and that only wrenches with negligible contact moment occur, which is a reasonable assumption for impulsive collisions, the translational and angular momentum can be exploited to isolate the contact. Indeed, considering $\boldsymbol{h}_c = [\boldsymbol{h}_c^{t\,T}\ \boldsymbol{h}_c^{r\,T}]^T$, the second cardinal equation of dynamics can be written as

$$\frac{d\boldsymbol{h}_c^r}{dt} = \boldsymbol{m}_{ext,c} = \boldsymbol{p}_{wc} \times \boldsymbol{f}_{ext,c} = \boldsymbol{p}_{wc} \times \frac{d\boldsymbol{h}_c^t}{dt} \tag{6}$$

where $\boldsymbol{f}_{ext,c}, \boldsymbol{m}_{ext,c} \in \mathbb{R}^3$ are the components of the projection in C of $\boldsymbol{\mathcal{W}_{ext}}$ and $\boldsymbol{p}_{wc} \in \mathbb{R}^3$ is the position vector from frame C to the contact point. Integrating Eq. (6), under the assumptions previously stated, the following relation can be obtained:

$$\Delta\boldsymbol{h}_c^r = \boldsymbol{p}_{wc} \times \Delta\boldsymbol{h}_c^t \tag{7}$$

Hence, the contact point lies on the line

$$\boldsymbol{l}_w = \frac{\Delta\boldsymbol{h}_c^t \times \Delta\boldsymbol{h}_c^r}{||\Delta\boldsymbol{h}_c^t||^2} + k\Delta\boldsymbol{h}_c^t \in \mathbb{R}^3 \tag{8}$$

which passes through $\boldsymbol{p}_{wc}$ and has the same orientation of $\boldsymbol{f}_{ext,c}$.

Knowing $\boldsymbol{l}_w$ and the configuration of the space robot at the contact time, it is possible to find the contact point as the intersection between the line and the robot, whose representation could be simplified exploiting primitive shapes. In the unlucky case of multiple possible contact points, the type of the ongoing on-orbit operation could provide additional information to identify the most likely one. This method can be applied similarly also using $\boldsymbol{h}_i$.

6. Simulation example

A spacecraft equipped with a 3 DoF manipulator is considered. The kinematics and dynamics parameters of the free-floating robot are reported in Tab. 1. The system is initially stationary and the initial joint angles are $\boldsymbol{q}_0 = [-25\ 45\ 81]^T$ deg.

At time $t = 2$ s, first and third joint are commanded to follow a trapezoidal velocity profile to reach a maximum velocity of 0.075 rad/s and -0.015 rad/s, respectively, in 1 s. It should be noted that the joint control strategy is irrelevant for the proposed method. At time $t = 3.887$ s, the third link impacts another free-floating object, as shown in Fig. 2.

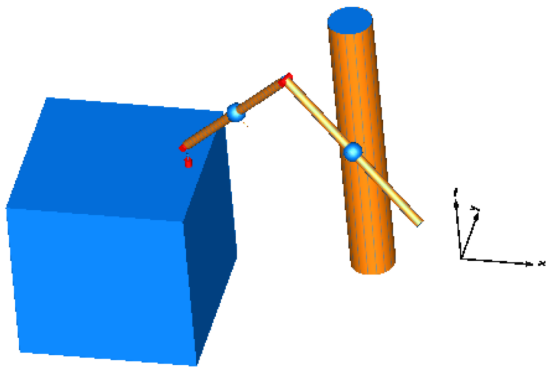

Fig. 2: Simulation scenario.

Table 1: Kinematics and dynamics parameters.

	l [m]	m [kg]	I_x [kgm^2]	I_y [kgm^2]	I_z [kgm^2]
Base	-	150	15.0	21.8	18.88
Link 1	0.17	3	0.03	0.03	0.03
Link 2	1.3	9	1.65	1.65	0.64
Link 3	1.3	6	0.25	0.25	0.03

Considering a local coordinate frame at both contact points (on the link and on the impacted object) with one axis normal to the surface, the normal component of the contact force is modeled as follows:

$$f_n = K\delta^m + D\delta^m\dot{\delta} \tag{9}$$

where $K = 2 \cdot 10^7$ and $D = 9 \cdot 10^4$ are the elastic and damping coefficient, δ is the penetration in the normal direction and, in the presented case, $m = 1.5$. The tangential components of the contact force are null since friction is neglected.

For the threshold approach the confidence parameter Γ_{th} is set equal to 6, while, for the ICI-CDT, Γ_{cdt} is set equal to 2 and N equal to 20.

Table 2: Noise parameters.

σ_{x_b} [mm]	1
σ_{v_b} [mm/s]	1
σ_ϕ [rad]	0.026
σ_q [rad]	$5 \cdot 10^{-5}$
$\sigma_{\dot{q}}$ [rad/s]	10^{-4}

The measurements of the angular velocity are simulated using Eq. (4) with standard deviations $\sigma_\omega =$

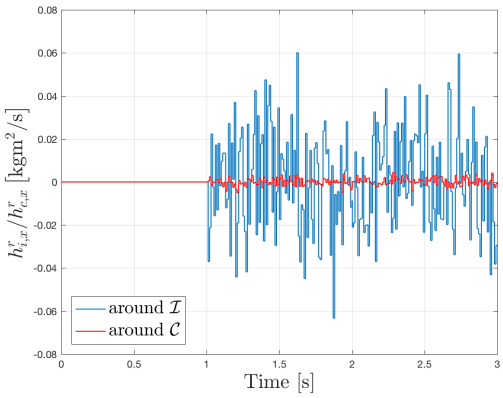

(a) Rotational momentum along x

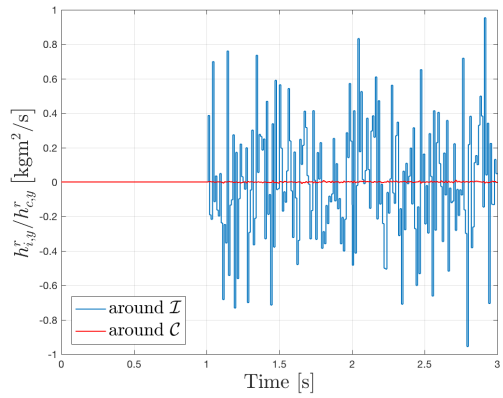

(b) Rotational momentum along y

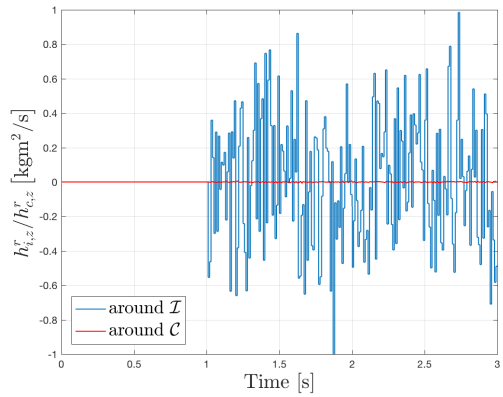

(c) Rotational momentum along z

Fig. 3: Effects of noise on the rotational momentum around $\mathcal{I}$ and $\mathcal{C}$.

$3.162 \cdot 10^{-4}$ µrad/s$^{3/2}$ and $\sigma_{b\omega} = 0.316$ µrad/s$^{1/2}$, and initial bias on each axis $b_{\omega,0} = 0.1$ deg/hr. The standard deviations of the Gaussian noise on the other measurements are reported in Tab. 2. $\boldsymbol{x}_b$ and $\boldsymbol{\phi}$ are the position and the Euler angles of the base. Measurement of the base position are required only to compute $\boldsymbol{h}_i$. An acquisition frequency of 100 Hz is considered.

Before proceeding with the simulation example, Fig. 3 shows the effects of noise on the components of the total momentum, explained in Sect. 4. At the beginning, an ideal condition is considered, then at time $t = 1$ s noise is switch on. Rotational momentum around $\mathcal{C}$ is less affected by noise than the one around $\mathcal{I}$, as expected. Therefore, $\boldsymbol{h}_c$ is used in the simulation example.

Fig. 4 shows the variation in the components of the total momentum after the collision. All the components of the momentum change due to the collision, except for the z-component of the translational momentum. Note the higher noisiness of the translational momentum, whose cause has been explained in Sect. 4. Both the ICI-CDT and threshold approach can detect a drift in the stationarity of the translational and rotational momentum, respectively. As expected, the threshold approach turns out to be prompter with a detection delay of few milliseconds, basically limited only by the acquisition frequency. On the other hand, in Fig. 4a the capability of the ICI-CDT of detecting variation comparable to the noise can be appreciated, even if with an increased delay. Detection performance closer to the threshold method can be achieved when changes are more sudden (see Fig. 4b).

Finally, as regards the isolation phase, the link involved in the collision is immediately identified, while the estimation of the point of application of the collision force requires few tens of milliseconds to converge (due to noise), as shown in Fig. 5. From the operational point of view, the mean value of the contact point is computed iteratively to filter some noise.

7. Conclusions and future works

In this paper collision handling problem for free-floating space robot has been addressed. First of all, a general overview of the problem has been provided. Then, some methods for collision detection and isolation based on monitoring the total momentum of the system have been proposed. The performance of the proposed strategies has been assessed through a simulation example, which has shown promising results. Further analysis will be carried out considering dif-

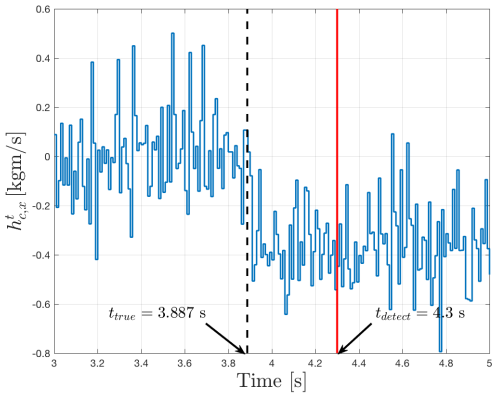

(a) Translational momentum along x

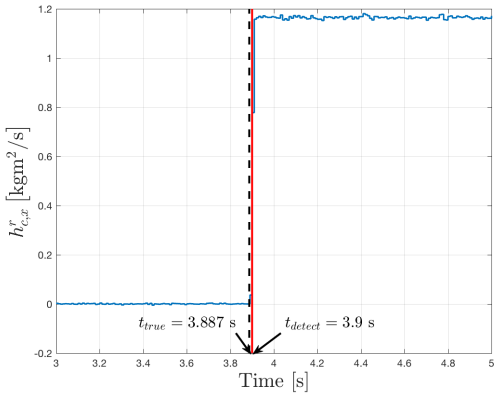

(b) Rotational momentum along x

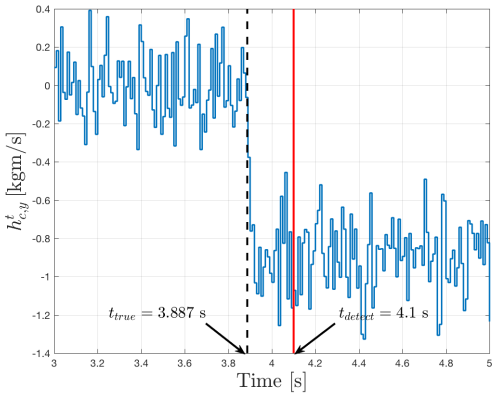

(c) Translational momentum along y

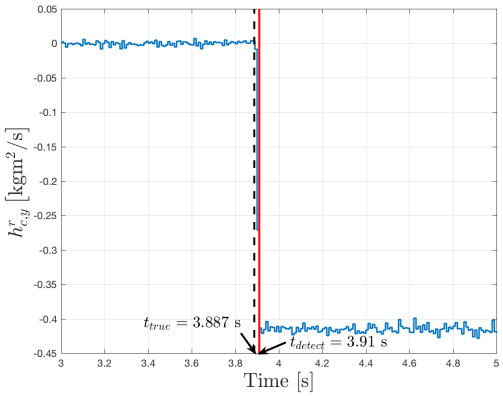

(d) Rotational momentum along y

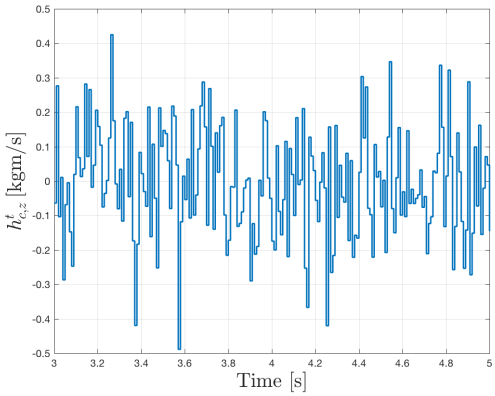

(e) Translational momentum along z

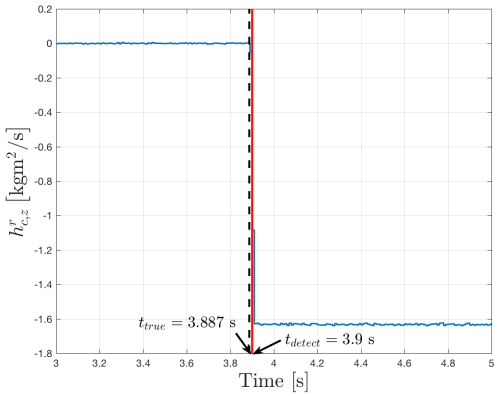

(f) Rotational momentum along z

Fig. 4: Variation in the components of the total momentum due to the collision.

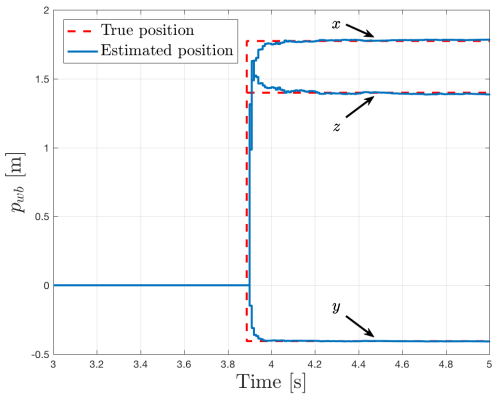

Fig. 5: Point of application of the collision force.

ferent level of intensity of the contact, different level of noise and uncertainties. Moreover, the methods will be extended to the controlled-base case.

Acknowledgements

The author F.C. thanks the Italian Space Agency (ASI) for sponsoring him to attend the 69th International Astronautical Congress in Bremen.

References

[1] R. Rembala and C. Ower, "Robotic assembly and maintenance of future space stations based on the ISS mission operations experience," *Acta Astronautica*, Vol. 65, No. 7-8, 2009, pp. 912–920.

[2] M. Oda, "Space robot experiments on NASDA's ETS-VII satellite-preliminary overview of the experiment results," *Robotics and Automation, 1999. Proceedings. 1999 IEEE International Conference on*, Vol. 2, IEEE, 1999, pp. 1390–1395.

[3] A. Ogilvie, J. Allport, M. Hannah, and J. Lymer, "Autonomous satellite servicing using the orbital express demonstration manipulator system," *Proc. of the 9th International Symposium on Artificial Intelligence, Robotics and Automation in Space (i-SAIRAS'08)*, 2008, pp. 25–29.

[4] B. Siciliano and O. Khatib, *Springer handbook of robotics*. Springer, 2016.

[5] A. Flores-Abad, O. Ma, K. Pham, and S. Ulrich, "A review of space robotics technologies for on-orbit servicing," *Progress in Aerospace Sciences*, Vol. 68, 2014, pp. 1–26.

[6] A. Flores-Abad, M. Nandayapa, and M. A. Garcia-Teran, "Force sensorless impedance control for a space robot to capture a satellite for on-orbit servicing," *2018 IEEE Aerospace Conference*, IEEE, 2018.

[7] S. A. A. Moosavian and E. Papadopoulos, "On the control of space free-flyers using multiple impedance control," *Robotics and Automation, 1997. Proceedings., 1997 IEEE International Conference on*, Vol. 1, IEEE, 1997, pp. 853–858.

[8] D. N. Nenchev and K. Yoshida, "Impact analysis and post-impact motion control issues of a free-floating space robot subject to a force impulse," *IEEE Transactions on Robotics and Automation*, Vol. 15, No. 3, 1999, pp. 548–557.

[9] S. Abiko, R. Lampariello, and G. Hirzinger, "Impedance control for a free-floating robot in the grasping of a tumbling target with parameter uncertainty," *Intelligent Robots and Systems, 2006 IEEE/RSJ International Conference on*, IEEE, 2006, pp. 1020–1025.

[10] S. Yoshikawa and K. Yamada, "Impact estimation of a space robot at capturing a target," *Intelligent Robots and Systems' 94.'Advanced Robotic Systems and the Real World', IROS'94. Proceedings of the IEEE/RSJ/GI International Conference on*, Vol. 3, IEEE, 1994, pp. 1570–1577.

[11] S. Haddadin, A. De Luca, and A. Albu-Schäffer, "Robot collisions: A survey on detection, isolation, and identification," *IEEE Transactions on Robotics*, Vol. 33, No. 6, 2017, pp. 1292–1312.

[12] C. Alippi, G. Boracchi, and M. Roveri, "Change detection tests using the ICI rule," *Neural Networks (IJCNN), The 2010 International Joint Conference on*, IEEE, 2010, pp. 1–7.

[13] J. L. Crassidis and F. L. Markley, "Unscented filtering for spacecraft attitude estimation," *Journal of guidance, control, and dynamics*, Vol. 26, No. 4, 2003, pp. 536–542.

[14] A. Goldenshluger and A. Nemirovski, "On spatially adaptive estimation of nonparametric regression," *Mathematical methods of Statistics*, Vol. 6, No. 2, 1997, pp. 135–170.